

THEORETICAL COMPUTATION OF A STRESS FIELD IN A CYLINDRICAL GLASS SPECIMEN

JÚLIUS HODOŇ, MAREK LIŠKA, NORBERT KREČMER*

*Vitrum Laugaricio - Joint Glass Center, of IIC SAS, TnU AD, FChPT STU and RONA,
Trencin SK-911 50, Slovak Republic*

**RONA, j.s.c., Lednické Rovne, SK-020 61, Slovak Republic*

E-mail: julius.hodon@tnuni.sk

Submitted September 27, 2010; accepted March 27, 2011

Keywords: Mechanical stress, Numerical model, Structural relaxation, Stress relaxation, Thermoelasticity

This work deals with the computation of the stress field generated in an infinitely high glass cylinder while cooling. The theory of structural relaxation is used in order to compute the heat capacity, the thermal expansion coefficient, and the viscosity. The relaxation of the stress components is solved in the frame of the Maxwell viscoelasticity model. The obtained results were verified by the sensitivity analysis and compared with some experimental data.

INTRODUCTION

Mechanical stress is a frequently discussed physical quantity in the glass industry. Articles become fragile under the stress influence, their lifetime and safety decreases, they crack. The process of stress generation is a complex and still opened issue. The methodology of measurement enables only to measure the differences of the principal stresses.

This work describes various ways of stress computation in specimens with cylindrical symmetry. The computation of the axial stress component is realized by an integral expression adopted from a literature as well as by using an alternative model. Material parameters such as the viscosity, the heat capacity and the thermal expansion are taken as functions of the thermodynamic and the fictive temperature. The algorithm consists of the heat conduction model, model of the structural relaxation and the stress relaxation.

METHOD

The heat conduction model

A time progression of the temperature field along the radius of the glass specimen is needed in order to calculate the stress. The computation starts from the heat conduction differential equation in the polar coordinate system:

$$c_{pf}(T, T_f) \cdot \rho \left(\frac{\partial T}{\partial t} \right)_r = \lambda \left[\left(\frac{\partial^2 T}{\partial r^2} \right)_t + \frac{1}{r} \left(\frac{\partial T}{\partial r} \right)_t \right] + \left(\frac{\partial \lambda}{\partial r} \right)_t \left(\frac{\partial T}{\partial r} \right)_t \quad (1)$$

derived from the heat balance of the cylindrical element ($r+dr$) per time dt , where ρ represents the density and λ is the heat conductivity. The heat capacity c_{pf} is expressed [1, 2] as a function of the thermodynamic temperature T , and the fictive temperature T_f :

$$c_{pf} = c_{pg} + (c_{pm} - c_{pg}) \frac{dT_f}{dT} \quad (2)$$

where c_{pg} represents the heat capacity of the glass and c_{pm} is the heat capacity of the metastable melt. Both quantities were measured by DSC ($c_{pg} = 1.3 \pm 0.13$ J/gK, $c_{pm} = 1.6 \pm 0.16$ J/gK). Thus, the computation of heat conduction must be interconnected with the computation of structural relaxation, which gives the time dependence of the T_f .

The heat flow through the bases is equal to zero; therefore, in this context we consider the glass specimen as infinitely high. The differential Equation (1) can be solved in the assumption of the validity of the Robin boundary condition of the third kind [3]:

$$a(T_{\text{surface}} - T_{\text{surroundings}}) = -\lambda \left(\frac{\partial T}{\partial r} \right)_{r=R,t} \quad (3)$$

where a is the heat transfer coefficient. By using the finite difference method, the differential Equation (1) is transformed into the difference equation in the explicit shape. In this shape, we are able to reach the temperature

in specific nodal point directly by using the temperature that has been obtained in the previous time step.

The temperature history is computed in listed style in single nodes along the radius of the specimen. This history is saved in a matrix and thereafter used in following computations.

The structural relaxation model

The computation of the Tool fictive temperature T_f starts at a temperature above the glass transition temperature T_g at the condition of the metastable equilibrium ($T_f=T$). The time continuation of T_f was obtained in the Tool-Narayanaswamy-Mazurin (TNMa) model of the structural relaxation by solving the Equation [1]:

$$T_f(t) = T(t) - \int_0^t dt' \left(\frac{dT}{dt} \right) M[\xi(t) - \xi(t')] \quad (4)$$

where M is the Kohlrausch-Williams-Watt relaxation function, t is time and ξ is the non-dimensional reduced time. The relaxation function M is expressed by the formula:

$$M(\xi) = \exp(-\xi^b) \quad (5)$$

where the parameter b determines the width distribution of the relaxation times $0 < b \leq 1$. The non-dimensional reduced time ξ is determined:

$$\xi(t) = \int_0^t \frac{dt'}{\tau(t')} = \int_0^t \frac{K}{\eta(t')} dt' \quad (6)$$

where K is an elastic constant and η is the dynamic viscosity. For the computation of the reduced time, the viscosity according to Mazurin is needed [2]:

$$\log \eta(T, T_f) = \left(A + \frac{B}{T_f - T_0} \right) \frac{T_f}{T} + \log \eta_0 \left(1 - \frac{T_f}{T} \right) \quad (7)$$

These relations (4-7) were used in order to obtain the progression of the fictive temperature in each time and space step. The single model parameters (Table 1)

Table 1. Material parameters of the barium crystal glass (TNMa model) [4].

Parameter	Value
$\log(K/\text{dPa})$	9.59 ± 0.07
b	0.548 ± 0.017
$\log(\eta_0/\text{dPa.s})$	1.02 ± 0.22
$10^7 \alpha_g/\text{K}^{-1}$	101.0 ± 4.9
$10^7 \alpha_m/\text{K}^{-1}$	347.1 ± 2.4

were gained by using the nonlinear regression analysis of thermomechanic data of the barium crystal glass [4].

The stress generation model

The temperature gradient generates the radial, tangential and axial stress components, which can be obtained by the following Equations [5]:

$$\sigma_r(r) = \frac{E}{1-\nu} \left(\frac{1}{R^2} \int_0^R \alpha_f T r dr - \frac{1}{r^2} \int_0^r \alpha_f T r dr \right) \quad (8)$$

$$\sigma_t(r) = \frac{E}{1-\nu} \left(\frac{1}{R^2} \int_0^R \alpha_f T r dr + \frac{1}{r^2} \int_0^r \alpha_f T r dr - \alpha_f T(r) \right) \quad (9)$$

$$\sigma_a(r) = \frac{E}{1-\nu} \left(\frac{2}{R^2} \int_0^R \alpha_f T r dr - \alpha_f T(r) \right) \quad (10)$$

where ν represents the Poisson ratio and E is the Young's modulus. The coefficient of thermal expansion α_f depends on T and T_f as well as c_{pf} in the Equation (2):

$$\alpha_f = \alpha_g + \Delta\alpha \frac{dT_f}{dT} \quad (11)$$

where $\Delta\alpha = \alpha_m - \alpha_g$, which is the difference between the thermal expansion of metastable melt and glass. The temperature field was described by the symmetrical polynomial equation of the 4th degree

$$T(r) = T_0 + T_2 r^2 + T_4 r^4 \quad (12)$$

which properly describes the radial course of the temperature field. Under this assumption, the integration of Equations (8 - 10) leads to more convenient shapes for calculations. Cooling of the i -indexed element (Figure 1) starts from the zero time step ($n=0$), where the residual stresses equal to zero

$$\sigma_{i,n=0}^{\text{rez}} = 0 \quad (13)$$

For the computation of the residual stress in the following time steps is necessary to know the value of the term

$$\Delta\sigma_{i,n} = (\sigma_{i,n} - \sigma_{i,n-1}), \quad (14)$$

which is the difference between the stresses obtained from the Equations (8-10) in the present and previous time step. Then, the final residual stress is expressed by the equation

$$\Delta\sigma_{i,n}^{\text{rez}} = (\sigma_{i,n-1}^{\text{rez}} + \Delta\sigma_{i,n}) \exp\left(-\frac{\Delta TE}{2\eta(T_{i,n}, T_{f,i,n})}\right) \quad (15)$$

The discrete stress generation model

Alternatively, own discrete model was used in order to calculate the axial residual stress. The calculation is based on the thermal deformation of the discrete elements with shape sketched in the (Figure 1).

For each element indexed i in the time step indexed j is:

$$l_{i,j} = l_{i,j-1} (\alpha_g \Delta T_{i,j} + \Delta \alpha \Delta T_{i,j} + 1) \quad (16)$$

From the condition of mechanical equilibrium:

$$\sum_{i=1}^N F_i = 0 \quad (17)$$

we see that the relation of the common equilibrium height is:

$$\bar{l}_j = \frac{\sum_{i=1}^N S_i}{\sum_{i=1}^N S_i / l_{i,j}} \quad (18)$$

where S_i represents the base area of the i indexed circular ring (Figure 2).

Each element is stretched or pressed with respect to the equilibrium height by various magnitudes. These deformation differences evoke the tensile or compressive stress. There is a viscosity change of axial deformation under the stress influence during the time interval Δt :

$$\Delta l_{i,j} = (l_{i,j} - \bar{l}_j) \exp\left(-\frac{\Delta t E}{2\eta(T_{i,n}, T_{i,i,n})}\right) \quad (19)$$

Finally, the residual stress is gained by using the

$$\sigma_{i,n}^{rez} = E \Delta l_{i,j} / \bar{l}_j$$

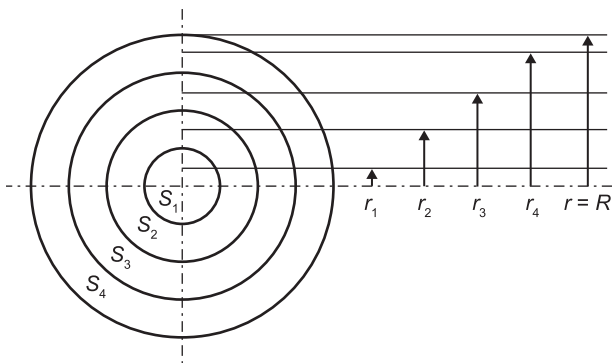


Figure 1. Discrete element shapes of the cylinder, where S is the base area and r is the radius of i -indexed element.

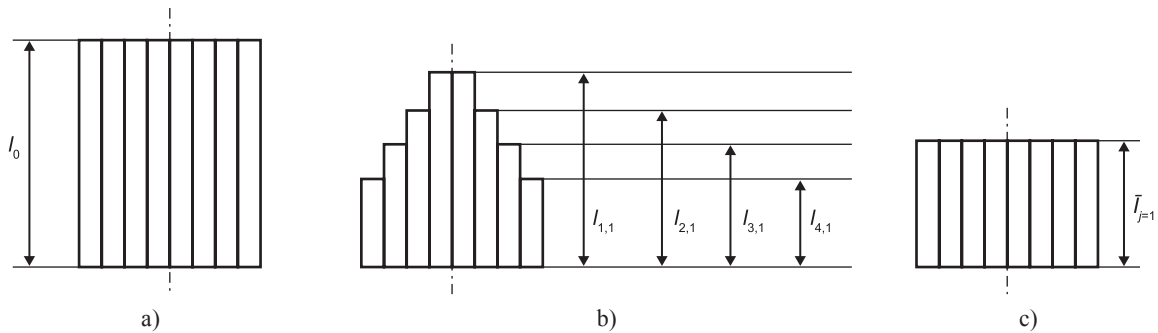


Figure 2. a) space elements; b) element deformation under the shift of the temperature gradient influence; c) resultant deformation of the specimen.

Hook's law:

$$(20)$$

RESULTS AND DISCUSSION

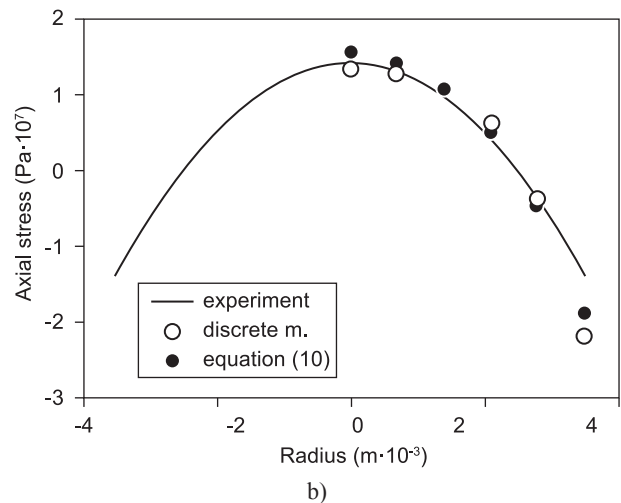
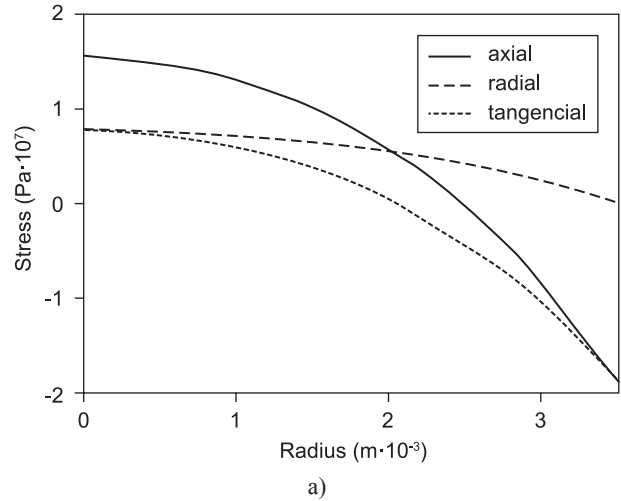


Figure 3. a) stress components progressions according to the Equation (10); b) experimental data comparison of the axial stress component models

The progression of the stress components calculated by using the Equations (8-10) can be seen in the Figure 3a). We used the Poisson ratio equal to zero $\nu = 0$ and the heat transfer coefficient $a = 100 \text{ W} \cdot \text{m}^{-2} \cdot \text{K}^{-1}$. Figure 3b) compares the axial stress component computed by both listed ways with experimental data obtained by separation of the principal stress components according to the publication [6]. There was a glass cylinder ($R = 35 \text{ mm}$) used for the experiment, which was cooled freely on air at the temperature $T = 80^\circ\text{C}$. From the figure results, that the integral, as well as the discrete model give almost equivalent values. Even

more important fact is that these models perfectly fit the experimental data, whereby a practical utilization was proved.

The time progression of the stress generation in the surface node by using the discrete model is shown in the Figure 4. At this type of annealing, the generation of the temperature stress as well as the structural stress progresses parallel so the stress creation has a smooth continuance.

Sensitivity analyses for the influence of the heat transfer coefficient and the number of nodes p were

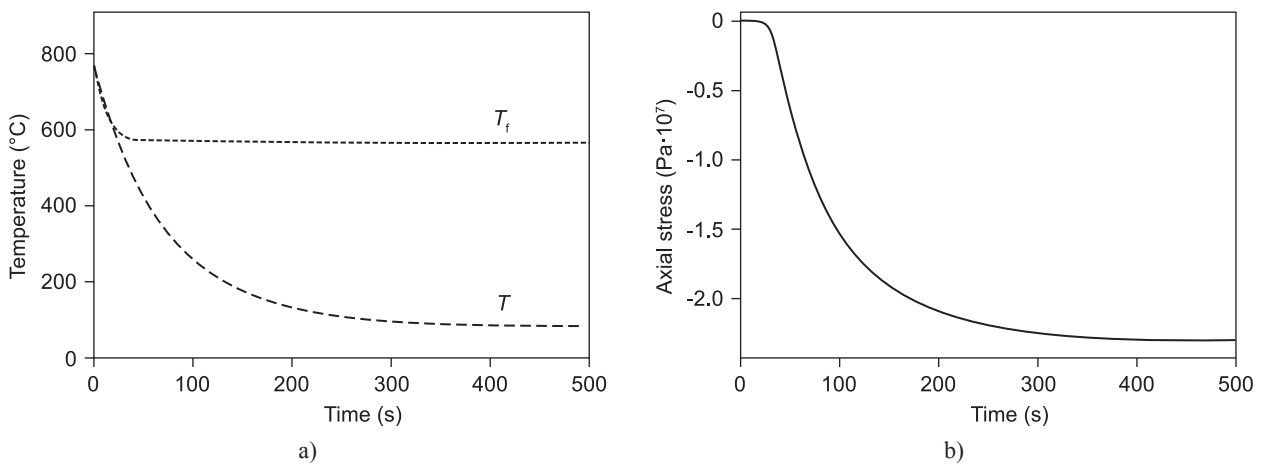


Figure 4. Surface axial stress evolution while cooling on air.

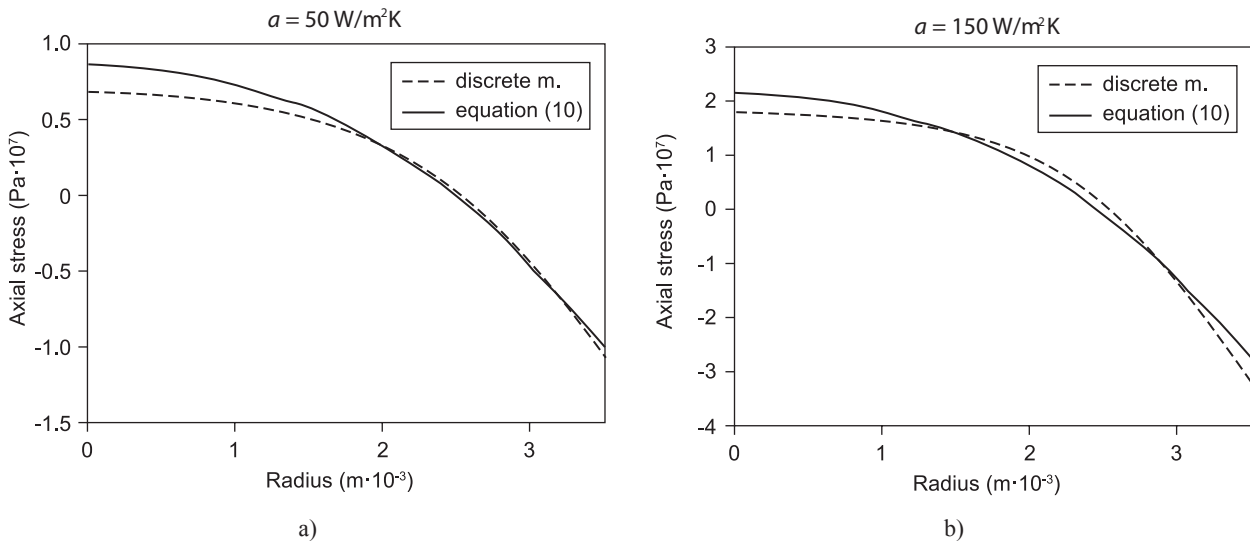


Figure 5. Arbitration of the algorithm sensitivity for the heat transfer coefficient ($\Delta t = 0.5 \text{ s}$, $p = 6$).

Table 2. Algorithm sensitivity for the number of nodes.

r (mm)	$p = 6$		$p = 8$		$p = 10$	
	0	3.5	0	3.5	0	3.5
σ_a (Pa) - discrete m.	2.90×10^7	-4.84×10^7	3.26×10^7	-4.66×10^7	3.39×10^7	-4.56×10^7
σ_a (Pa) - Equation (10)	3.49×10^7	-4.64×10^7	3.52×10^7	-4.48×10^7	3.58×10^7	-4.36×10^7
$M_{i=p,j=1}$	6.5121		3.3225		2.0099	

performed on both of these models. As the value of the coefficient a increases, the magnitude of residual stress does too (Figure 5).

The sensitivity of the algorithm for the number of nodes along the radius was performed under the conditions $a = 200 \text{ W.m}^{-2}\text{.K}^{-1}$, $\Delta t = 0,2 \text{ s}$ and $p = 6, 8, 10$. The values of the axial components of residual stress for center and surface of the cylinder are listed in the Table 2. There is no need to perform the time step sensitivity analysis because the time and space step are linked together by the Fourier dimensionless criteria:

$$M_{i,j} = \frac{\rho(T_{i,j})c_{pt}(T_{i,j})(\Delta r)^2}{\lambda(T_{i,j})\Delta t} \quad (21)$$

where Δr is the length of the space step. The numerical stability of the solution is safeguarded by the fulfillment of the condition $M > 2$ for each pair of indexes i and j [3].

It can be seen that the sensitivity of both of the models is sufficiently low. Results were reached with the aid of our own software made by the programming language MATLAB®.

CONCLUSION

The integral model adopted from literature, as well as own discrete model were developed for the calculation of the axial stress component. Both models were successfully verified by comparing with the experimental data. Sufficiently low sensitivity with

respect to the chosen parameters was demonstrated. The potential utilization of gained results is in the annealing process optimization. In the next work, the discrete model will be expanded into the new shape with all the stress components and implemented Poisson ratio.

Acknowledgement

This work was supported by Agency for Promotion Research and Development under the contract SUSPP-0006-09, by the Slovak Grant Agency for Science under the grant VEGA 1/0330/09. This publication was created in the frame of the project PVTECHSKLO, ITMS code 26220220072, of the Operational Program Research and Development funded from the European Fund of Regional Development.

References

1. Narayanaswami O.S.: J. Amer. Ceram. Soc. 54, 491 (1971).
2. Mazurin O.V.: *Steklovanie*, Nauka 1986 (In Russian).
3. Steidl H. et al.: *Úvod do proudění tekutin a sdílení tepla*. First edition, SNTL, Prague 1975 (In Czech).
4. Chromčíková M., Dej P.: *Ceramics – Silikáty* 50, 125 (2006).
5. Timoshenko, S., P., Goodier, J., N.: *Theory of Elasticity I, II*. Third edition. McGraw-Hill book Company, London 1970.
6. Krečmer N., Liška M., Chocholoušek J., Vrábek P.: *Ceramics – Silikáty* 52, 183 (2008).